

## Electronic Supplementary Information (ESI)

### Mechanoluminescence from pure hydrocarbon AIEgen

Yujun Xie, Jin Tu, Tianqi Zhang, Jiaqiang Wang, Zongliang Xie, Zhenguo Chi, Qian

Peng, Zhen Li\*

#### Table of Content

1. General method, computational study and materials	S2
2. Synthesis and characterization	
Synthesis of DTEBP, TTTPE and TETPE	S2-S3
Scheme S1. Synthesis route of TETPE	S2
3. Fig. S1. The previous reported luminophor with the properties of AIE and ML	S4
4. Fig. S2. Thermogravimetric analysis (TGA) curves of the TETPE	S4
5. Fig. S3. UV-vis absorption and PL spectra in different water/THF fraction mixtures	S4
6. Fig. S4. The PL decay curves of TETPE in different water/THF fraction mixtures	S5
7. Fig. S5. The fluorescence and phosphorescence of TETPE in THF solution at 77 K	S5
8. Fig. S6. X-ray diffraction (XRD) spectra of TETPE	S6
9. Table S1. Single crystal data of TETPE	S6
10. Fig. S7. The optimized geometry and frontier orbitals of TETPE in gas phase	S7
11. Table S2. The transition properties of TETPE	S7
12. Fig. S8. The molecular packing character of four dimers	S7
13. Table S3. The HOMO and LUMO energy level of dimer1-4	S8
14. Fig. S9. <sup>1</sup> H NMR spectrum of DTEBP	S8
15. Fig. S10. <sup>13</sup> C NMR spectrum of DTEBP	S9
16. Fig. S11. <sup>1</sup> H NMR spectrum of TETPE	S9
17. Fig. S12. <sup>13</sup> C NMR spectrum of TETPE	S10

## General methods

$^1\text{H}$  and  $^{13}\text{C}$  NMR spectra were measured on a MECUYRVX300 spectrometer. Mass spectra were measured on a ZAB 3F-HF spectrophotometer. Elemental analyses of carbon, hydrogen, and nitrogen were performed on a CARLOERBA-1106 microanalyzer. UV-vis absorption spectra were recorded on a Shimadzu UV-2500 recording spectrophotometer. Photoluminescence spectra were recorded on a Hitachi F-4600 fluorescence spectrophotometer. Fluorescence quantum yields were determined with a Hamamatsu C11347 Quantaaurus-QY absolute fluorescence quantum yield spectrometer. Fluorescence lifetimes were determined with a Hamamatsu C11367-11 Quantaaurus-Tau time-resolved spectrometer. The powder X-ray diffraction patterns of crystals were recorded by Rigaku MiniFlex 600 with an X-ray source of Cu  $K\alpha$  ( $\lambda=1.5418 \text{ \AA}$ ) at  $25 \text{ }^\circ\text{C}$  at 40 KV and 15 mA at a scan rate of  $5^\circ(2\theta)/\text{min}$  (scan range: 2-50  $^\circ$ ). The single-crystal X-ray diffraction data was collected in a Bruker Smart Apex CCD diffractometer.

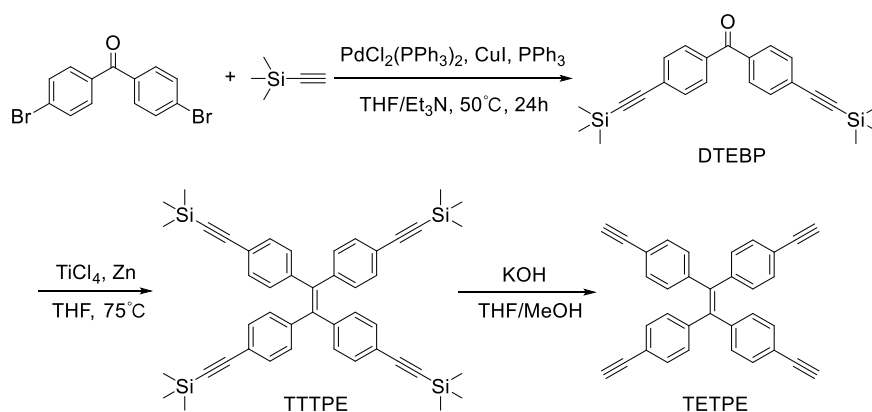
## Computational study

(TD)DFT calculations were performed on Gaussian 09 program (Revision D09).<sup>1</sup> The ground state ( $S_0$ ) geometries were optimized with the Becke's three-parameter exchange functional along with the Lee Yang Parr's correlation functional (B3LYP) using 6-31G(d) basis sets. The excitation energies in the first singlet state of monomers were obtained using the TD-DFT method based on an optimized molecular structure at ground state ( $S_0$ ).

## Materials

All solvents and reagents were purchased and used as received without further purification, unless otherwise mentioned. THF was dried over sodium-potassium alloy and distilled under argon atmosphere. Triethylamine (TEA) was bubbled with dry nitrogen.

## Synthesis and characterization



### Synthesis of DTEBP (bis(4-((trimethylsilyl)ethynyl)phenyl)methanone)

4,4'-Dibromobenzophenone (5.44 g, 16 mmol),  $\text{PdCl}_2(\text{PPh}_3)_2$  (450 mg, 0.64 mmol), CuI (244 mg, 1.28 mmol), and  $\text{PPh}_3$  (504 mg, 1.92 mmol) were added into a 250 mL Schlenk tube, and then the solvent of THF (85 mL) and TEA (40 mL) under nitrogen. After the reagents were dissolved, trimethylsilylacetylene (5.65 mL, 40 mmol) was injected. The solution was heated to  $50 \text{ }^\circ\text{C}$  and stirred 24 h. The formed solid was removed by filtration and washed with ethyl acetate. The filtrate was concentrated by evaporator under reduced pressure, and the crude product was purified by a column chromatography on silica gel with an ethyl acetate/petroleum ether mixture (1: 100 by

volume) as eluent. A white solid of DTEBP was obtained in an 84.6% yield (5.07 g).  $^1\text{H}$  NMR (400 MHz,  $\text{CDCl}_3$ )  $\delta$  (TMS, ppm): 7.72-7.70 (d,  $J=8.5$  Hz, 4H), 7.57-7.55 (d,  $J=8.5$  Hz, 4H), 0.27 (s, 18H).  $^{13}\text{C}$  NMR (100 MHz,  $\text{CDCl}_3$ )  $\delta$  (ppm): 195.36, 136.87, 132.01, 129.98, 127.64, 104.12, 98.20, and 0.00. MS,  $m/z$ : 374.10 ( $[\text{M}^+]$ , calcd for  $\text{C}_{23}\text{H}_{26}\text{OSi}_2$ , 374.63).

### Synthesis of TTTPE (1,1,2,2-tetrakis(4-((trimethylsilyl)ethynyl)phenyl)ethene)

Zinc powder (3.66 g, 56 mmol) was added into a 250 mL Schlenk tube, then the vessel was evacuated under vacuum and flushed with nitrogen for three times. 20 mL of THF was added and the mixture was cooled to 0 °C in an ice bath.  $\text{TiCl}_4$  (3.1 mL, 28 mmol) was added dropwise through a syringe. After stirred for 10 min, the mixture was warmed to reflux for 0.5 h. DTEBP (5.04g, 13.5 mmol) dissolved in THF (50 mL) with was injected, and the reaction lasted for 5 h. After cooled to room temperature, the reaction was quenched with diluted hydrochloric acid and then filtered. The filtrate was extracted with chloroform and the combined organic layer was dried over  $\text{Na}_2\text{SO}_4$ . The crude product was condensed by reduced evaporation and used for the next step directly without further purification and characterization.

### Synthesis of TETPE

Crude TTTPE and THF (40 mL) was added into a round-bottom flask, then KOH (1.3 g) in methanol (30 mL) was added. The mixture was stirred for overnight at room temperature. After the removal of the solvent by reduced evaporation, the crude product was exacted by DCM and washed with water. The organic layer was dried over  $\text{Na}_2\text{SO}_4$ , then the crude product was purified by a column chromatography on silica gel with a DCM/petroleum ether mixture (1: 50 by volume) as eluent. A pale-yellow solid of TETPE was obtained in a 77.9% yield (2.26 g) with two steps.  $^1\text{H}$  NMR (400 MHz,  $\text{DMSO}-d_6$ )  $\delta$  (ppm): 7.30-7.28 (d,  $J=8.4$  Hz, 8H), 6.95-6.93 (d,  $J=8.5$  Hz 8H), 3.07 (s, 4H).  $^{13}\text{C}$  NMR (100 MHz,  $\text{CDCl}_3$ )  $\delta$  (ppm): 143.29, 140.84, 131.81, 131.25, 120.69, 83.47 and 77.86. MS (EI),  $m/z$ : 428.32 ( $[\text{M}^+]$ , calcd for  $\text{C}_{34}\text{H}_{20}$ , 428.53). Anal. Calcd for  $\text{C}_{34}\text{H}_{20}$ : C, 95.30; H, 4.70. Found: C, 95.05; H, 4.86.

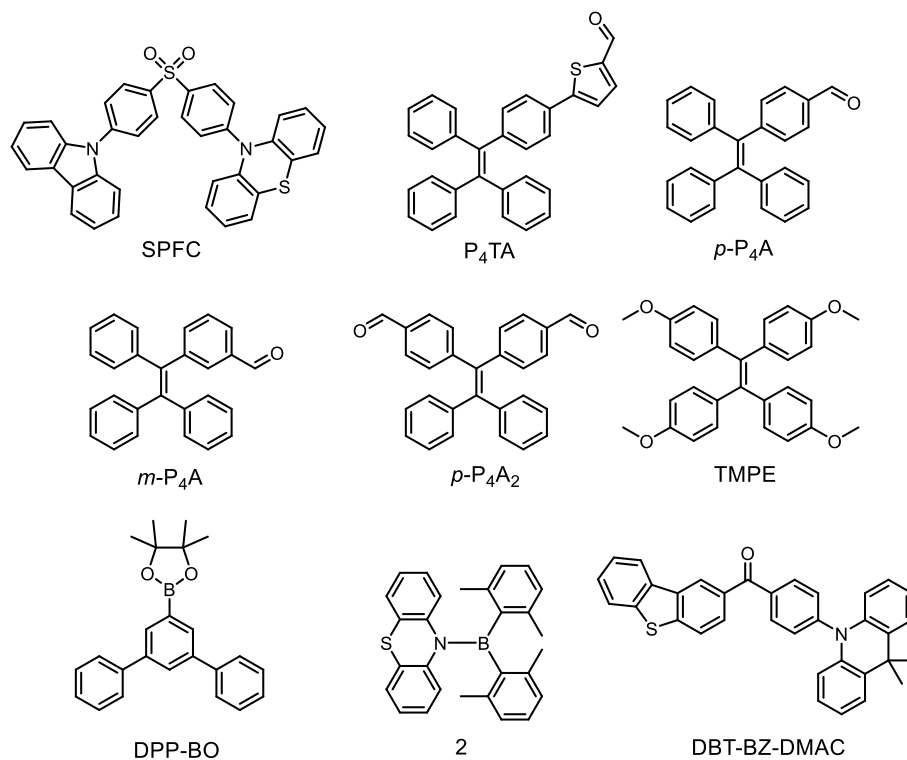


Fig. S1. The previous reported luminophor with the properties of AIE and ML.

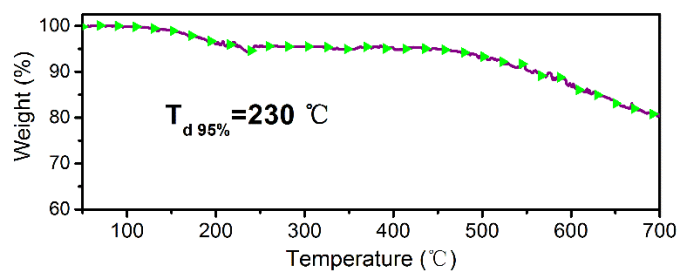


Fig. S2. Thermogravimetric analysis (TGA) curves of the TETPE.

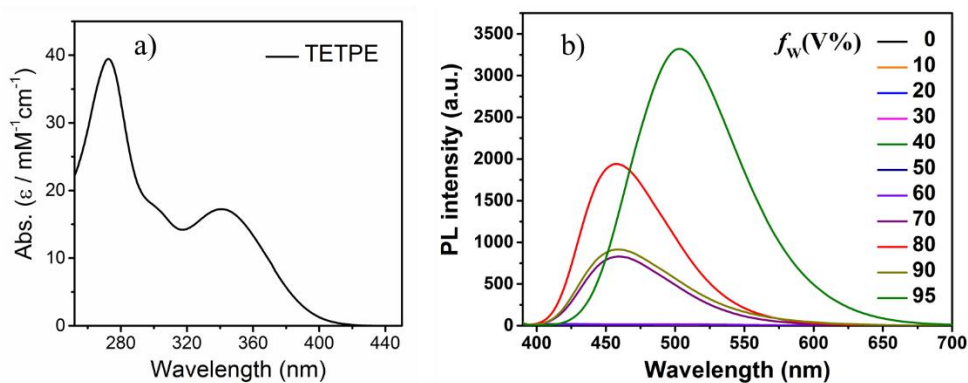


Fig. S3. (a) UV-vis absorption spectrum of TETPE in THF solution. (b) PL spectra of TETPE in different water/THF fraction ( $f_w$ ) mixtures under the excitation of 370 nm UV light. ( $c=85\ \mu\text{M}$ )

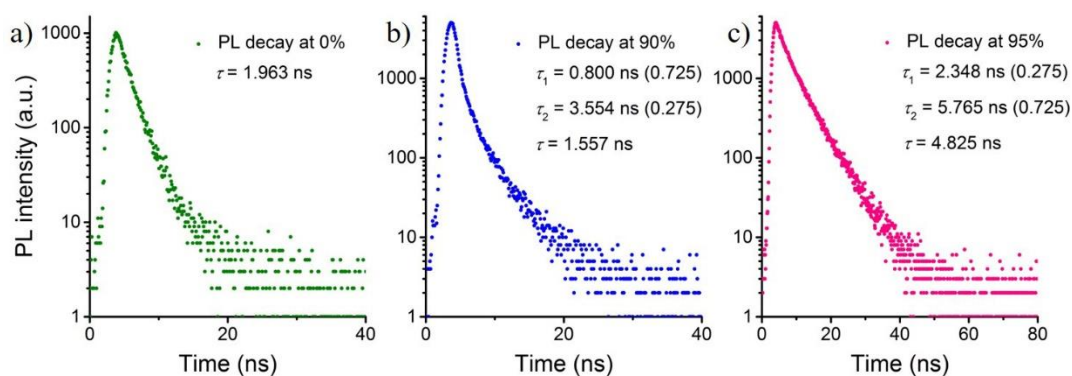


Fig. S4. The PL decay curves of TETPE in ratio of (a) 0%, (b) 90% and (c) 95% H<sub>2</sub>O/THF solution under the excitation of 370 nm UV light. (c=85 μM).

Table S1. The PL quantum yield ( $\Phi$ ) and lifetime ( $\tau$ ) of TETPE in ratio of (a) 0%, (b) 90% and (c) 95% H<sub>2</sub>O/THF solution (c=85 μM).

TETPE (H <sub>2</sub> O/THF)	$\Phi_{\text{PL}}$	$\tau$ (ns)
0%	Less than 1%*	1.963
90%	50.4%	1.557
95%	62.6%	4.825

\* Too small to be measured accurately.

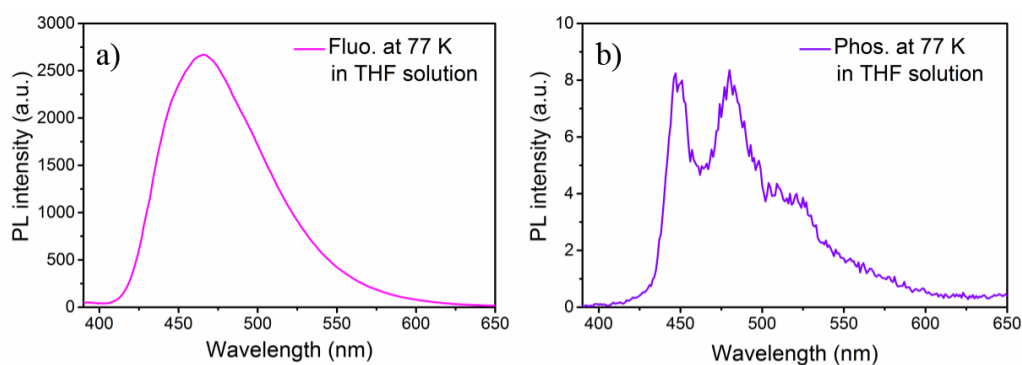


Fig. S5. The fluorescence (fluo.) and phosphorescence (phos.) of TETPE in THF solution at 77 K. (c=85 μM)

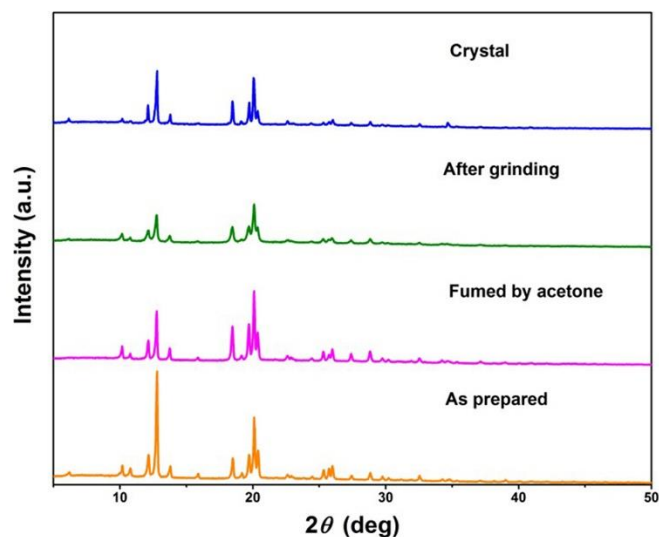
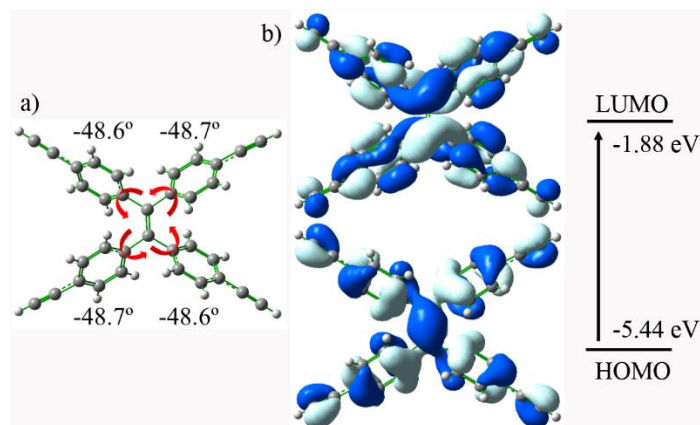


Fig. S6. X-ray diffraction (XRD) spectra of TETPE in crystal state, amorphous state (fine powder), the powder fumed by acetone and the as prepared state.

Table S2. Single crystal data of TETPE and the published TETPE crystal with CCDC number of 163147.

Name	TETPE	TETPE-163147
Formula	C <sub>34</sub> H <sub>20</sub>	C <sub>34</sub> H <sub>20</sub>
Wavelength (Å)	0.71073	0.71073
Crystal system	monoclinic	monoclinic
Space Group	C2	C2
Cell Length (Å)	a 16.519(8) b 8.812(4) c 11.140(10)	a 16.546(3) b 8.8418(18) c 11.178(2)
Cell Angle (°)	α 90.00 β 128.957(5) γ 90.00	α 90.00 β 129.00(3) γ 90.00
Cell Volume (Å <sup>3</sup> )	1261.0(14)	1270.9(4)
Z	2	2
Density (g/cm <sup>3</sup> )	1.129	1.120
F(000)	448	448
h <sub>max</sub> , k <sub>max</sub> , l <sub>max</sub>	20, 9, 13	22, 12, 14
T <sub>min</sub> , T <sub>max</sub>	0.9811, 0.9823	



**Fig. S7.** (a) The optimized geometry of TETPE in gas phase at b3lyp/6-31G\* level; (b) The corresponding frontier orbitals of TETPE.

Table S3. The first transition energy and corresponding molecular orbital contribution, oscillator strength ( $f$ ) of TETPE molecule in crystal phase and gas phase.

Phase	The first transition energy [eV]	Molecule orbital contribution	$f$
In crystal	3.53 (351 nm)	(HOMO $\rightarrow$ LUMO) 99.4%	0.4886
In gas	3.18 (390 nm)	(HOMO $\rightarrow$ LUMO) 99.7%	0.5590

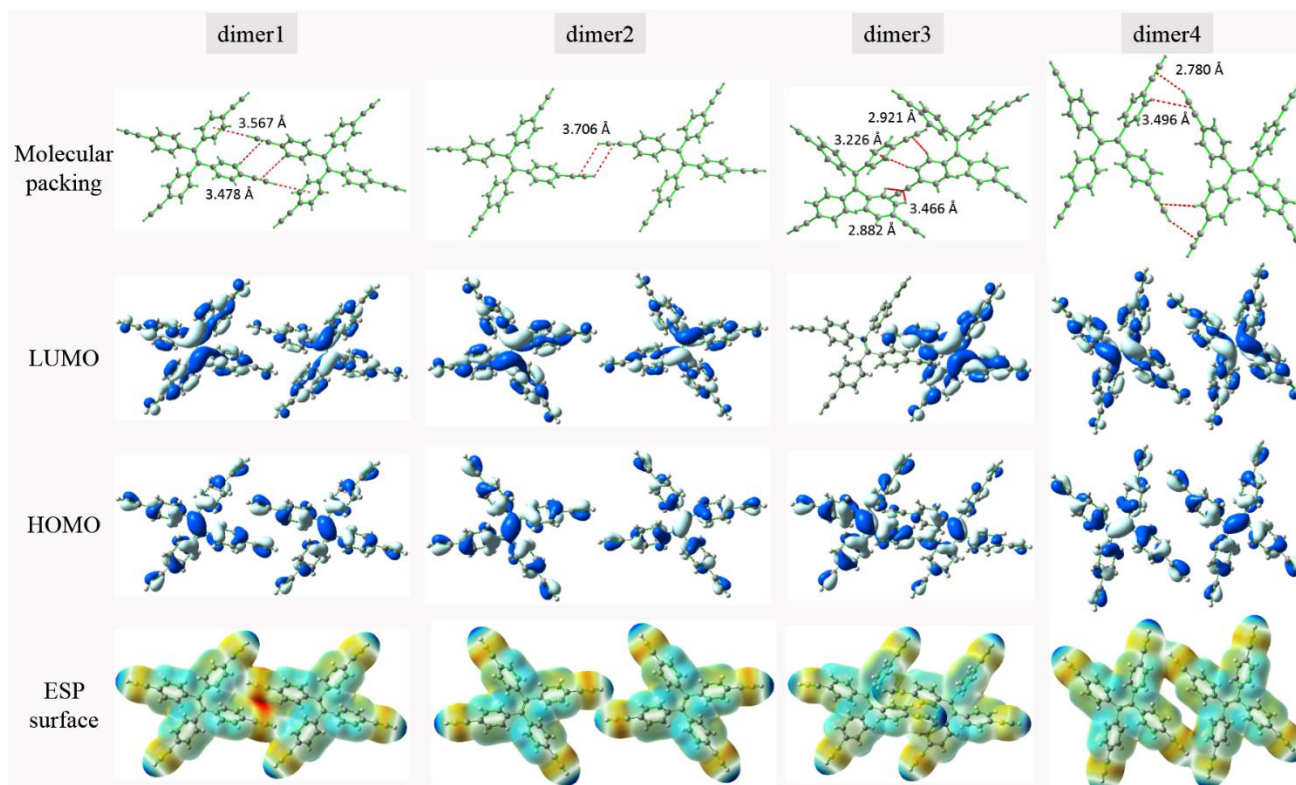


**Fig. S8.** The molecular packing arrangement, frontier orbital (HOMO and LUMO) and electrostatic potential (ESP) surface at 0.001 a.u. isosurface of electron density at b3lyp/6-31G\* level.

Table S4. The HOMO and LUMO energy level of dimer1-4.

	HOMO/eV	LUMO/eV
dimer1	-5.55	-1.60
dimer2	-5.57	-1.60
dimer3	-5.56	-1.60
dimer4	-5.53	-1.59

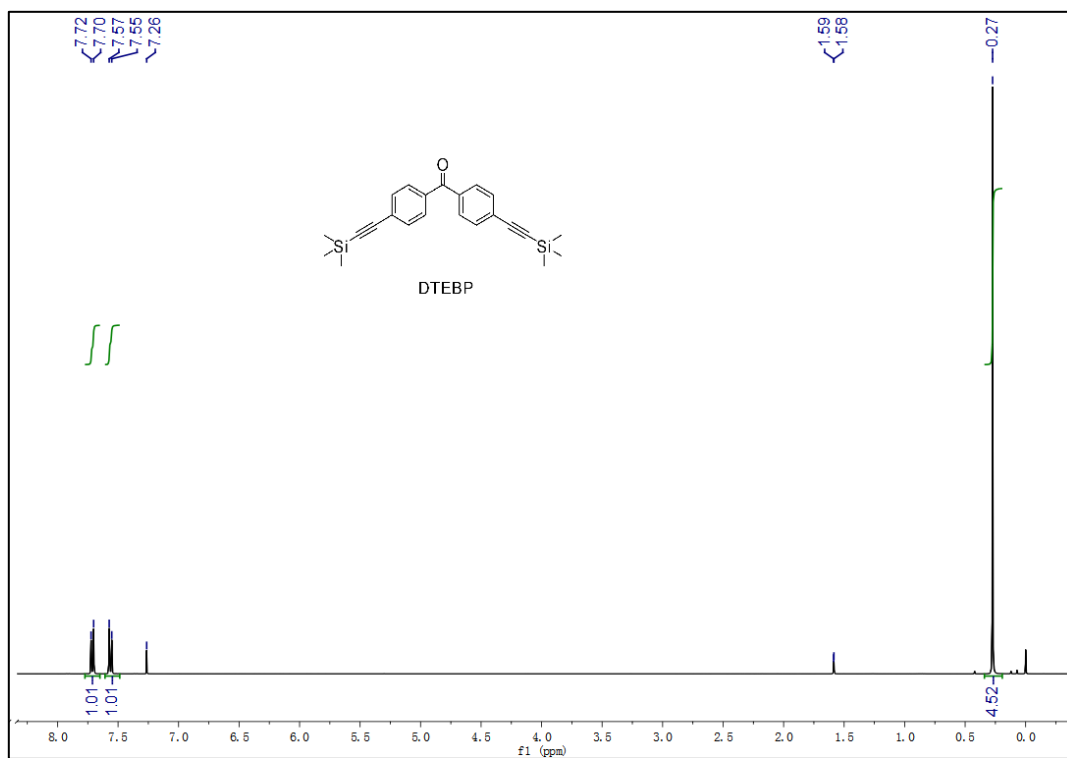


Fig. S9. <sup>1</sup>H NMR spectrum of DTEBP measured in CDCl<sub>3</sub>.



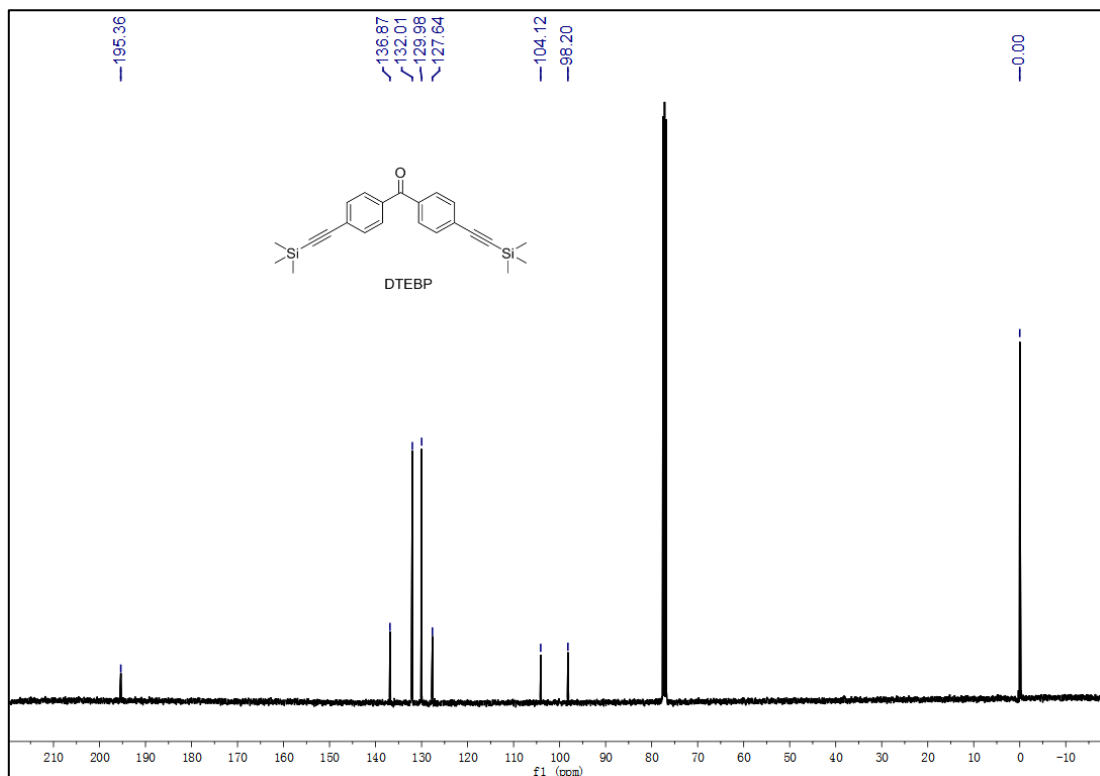


Fig. S10.  $^{13}\text{C}$  NMR spectrum of DTEBP measured in  $\text{CDCl}_3$ .

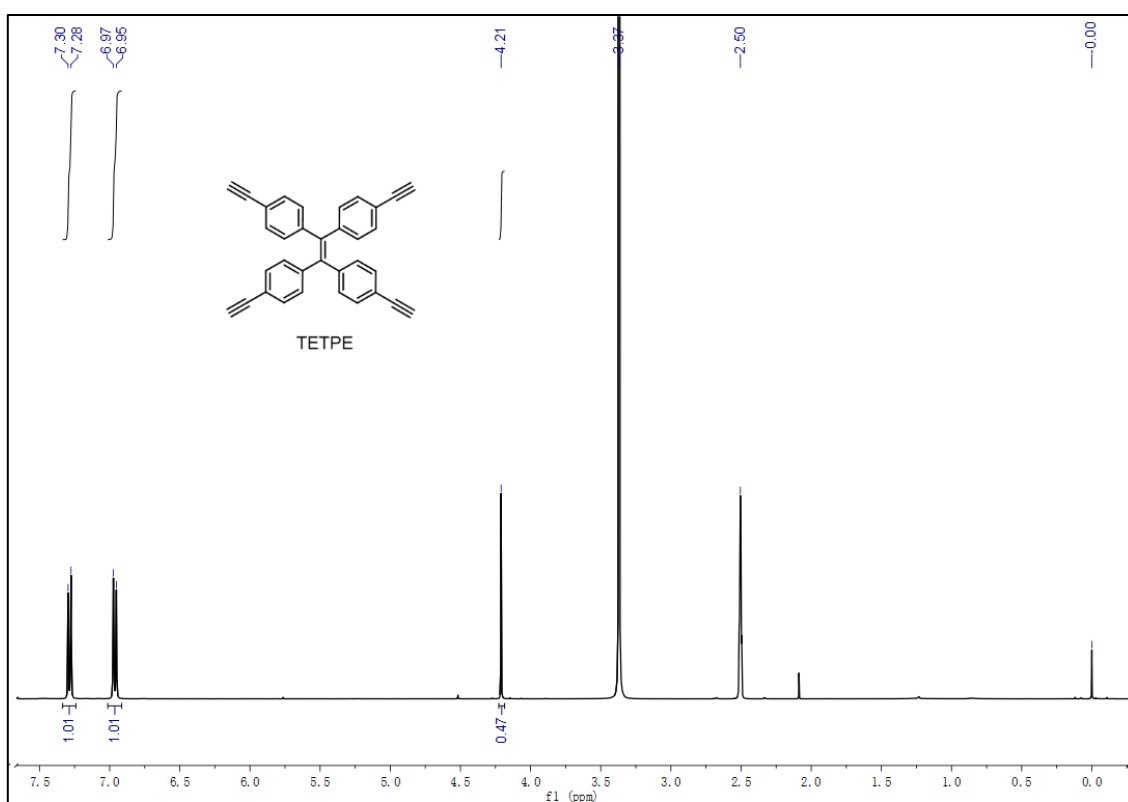


Fig. S11.  $^1\text{H}$  NMR spectrum of TETPE measured in  $\text{DMSO}-d_6$ .

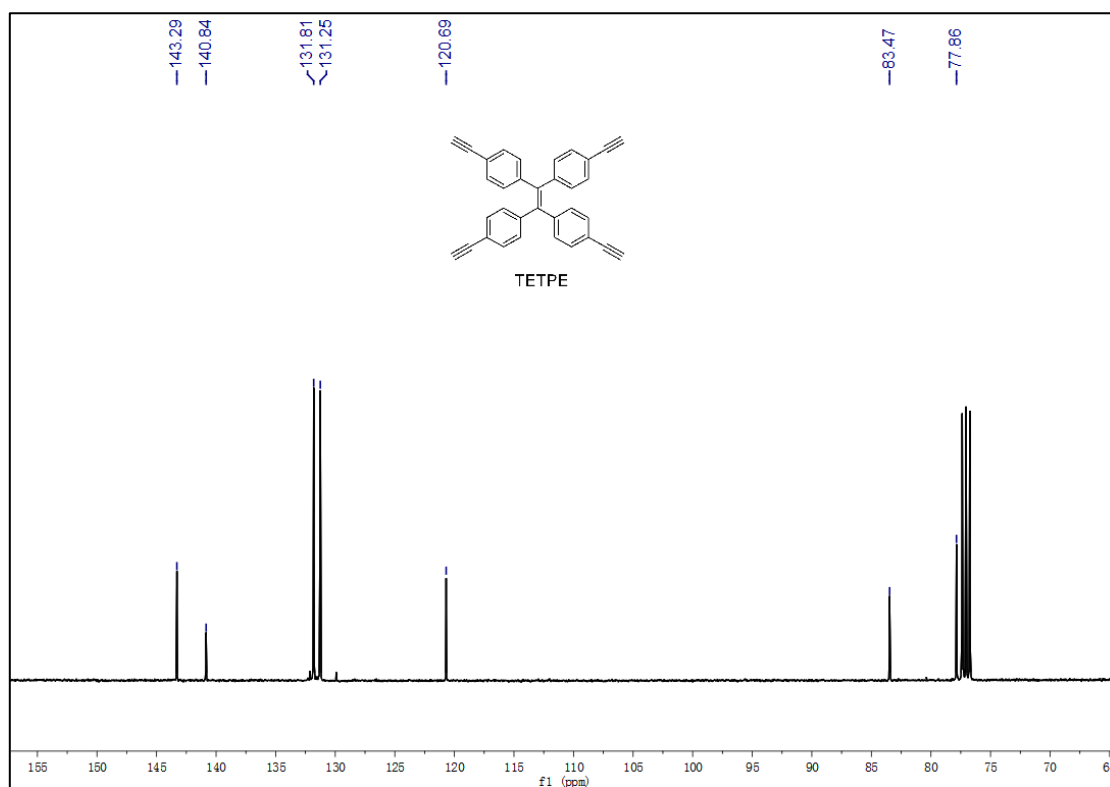


Fig. S12. <sup>13</sup>C NMR spectrum of TETPE measured in CDCl<sub>3</sub>.

## Reference

1. M. J. Frisch, G. W. Trucks, H. B. Schlegel, G. E. Scuseria, M. A. Robb, J. R. Cheeseman, G. Scalmani, V. Barone, B. Mennucci, G. A. Petersson, H. Nakatsuji, M. Caricato, X. Li, H. P. Hratchian, A. F. Izmaylov, J. Bloino, G. Zheng, J. L. Sonnenberg, M. Hada, M. Ehara, K. Toyota, R. Fukuda, J. Hasegawa, M. Ishida, T. Nakajima, Y. Honda, O. Kitao, H. Nakai, T. Vreven, J. A. Montgomery, Jr., J. E. Peralta, F. Ogliaro, M. Bearpark, J. J. Heyd, E. Brothers, K. N. Kudin, V. N. Staroverov, T. Keith, R. Kobayashi, J. Normand, K. Raghavachari, A. Rendell, J. C. Burant, S. S. Iyengar, J. Tomasi, M. Cossi, N. Rega, J. M. Millam, M. Klene, J. E. Knox, J. B. Cross, V. Bakken, C. Adamo, J. Jaramillo, R. Gomperts, R. E. Stratmann, O. Yazyev, A. J. Austin, R. Cammi, C. Pomelli, J. W. Ochterski, R. L. Martin, K. Morokuma, V. G. Zakrzewski, G. A. Voth, P. Salvador, J. J. Dannenberg, S. Dapprich, A. D. Daniels, O. Farkas, J. B. Foresman, J. V. Ortiz, J. Cioslowski, and D. J. Fox, Gaussian, Inc., Wallingford CT, 2013